

ARTICLE OPEN



Decreased thermal niche breadth as a trade-off of antibiotic resistance

Cristina M. Herren^{1,2,3} and Michael Baym^{1,2}

© The Author(s) 2022

Evolutionary theory predicts that adaptations, including antibiotic resistance, should come with associated fitness costs; yet, many resistance mutations seemingly contradict this prediction by inducing no growth rate deficit. However, most growth assays comparing sensitive and resistant strains have been performed under a narrow range of environmental conditions, which do not reflect the variety of contexts that a pathogenic bacterium might encounter when causing infection. We hypothesized that reduced niche breadth, defined as diminished growth across a diversity of environments, can be a cost of antibiotic resistance. Specifically, we test whether chloramphenicol-resistant *Escherichia coli* incur disproportionate growth deficits in novel thermal conditions. Here we show that chloramphenicol-resistant bacteria have greater fitness costs at novel temperatures than their antibiotic-sensitive ancestors. In several cases, we observed no resistance cost in growth rate at the historic temperature but saw diminished growth at warmer and colder temperatures. These results were consistent across various genetic mechanisms of resistance. Thus, we propose that decreased thermal niche breadth is an under-documented fitness cost of antibiotic resistance. Furthermore, these results demonstrate that the cost of antibiotic resistance shifts rapidly as the environment changes; these context-dependent resistance costs should select for the rapid gain and loss of resistance as an evolutionary strategy.

The ISME Journal (2022) 16:1843–1852; <https://doi.org/10.1038/s41396-022-01235-6>

INTRODUCTION

The extensive distribution of antibiotic-resistant bacteria across both clinical and environmental habitats demonstrates the difficulty of limiting the dispersion of antibiotic resistance [1]. However, evolutionary theory predicts that resistance should come with widespread fitness costs in the absence of antibiotics: if there were no cost, then all pathogens should become resistant, and resistance should never be lost [2–4]. Empirically, many known resistance mechanisms are energetically costly (e.g., efflux pumps), which divert a portion of a cell's energetic budget away from growth and reproduction [5, 6]. Many studies have sought to quantify fitness costs to antibiotic resistance with the goal of identifying growth deficits that accompany resistance (as reviewed by [7]). Meta-analyses of bacterial growth rates have found wide ranges of fitness costs for resistance to different antibiotics [8]. And, in some cases, there are no discernable growth rate difference between antibiotic-sensitive strains and resistant strains [9–11]. However, an important consideration is that most experimental tests of bacterial growth are done under tightly constrained environmental conditions, usually at 37 °C to mimic human body temperature. The absence of fitness cost in this single context does not preclude the presence of fitness costs in different conditions [12], meaning there may be unidentified fitness costs to these seemingly unaffected resistant bacteria.

Although bacterial cultures in the laboratory are maintained under a narrow range of environmental parameters, bacterial pathogens might encounter many different environments when

causing an infection [13, 14]. For instance, their host's body temperature might rise or fall [15], or the cell may have to persist outside the body during a transmission event [16]. Fitness costs to antibiotic resistance might manifest differently in these varied environments; for example, temperature mediates both antibiotic resistance and cell growth by affecting processes such as protein folding and the rate of chemical reactions within the cell [17, 18]. Thus, a mutation that confers resistance might be neutral at one temperature but could have adverse effects when protein shape or enzyme kinetics are altered. In this case, strong specialization for antibiotic resistance might have costs in the ability to tolerate multiple environments.

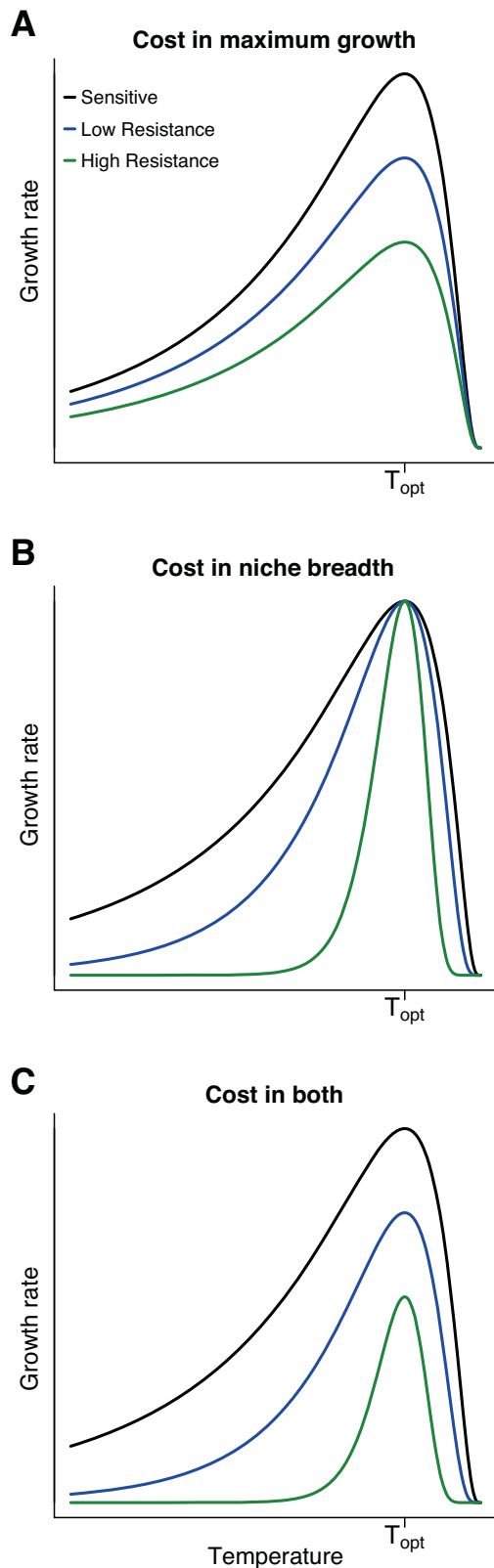
Here, we propose decreased thermal niche breadth, defined as reduced growth rate across a range of temperatures, as a cost of antibiotic resistance. Because niche breadth is independent of maximum growth rate, it is possible for fitness costs to manifest as either a cost in maximum growth rate (Fig. 1A), a cost in thermal niche breadth (Fig. 1B), or a cost in both maximum growth rate and thermal niche breadth (Fig. 1C). The addition of this dimension of fitness could reconcile the theoretical framework of requisite fitness costs with the experimental evidence that fitness costs are absent in some conditions; if costs to resistance are in decreased niche breadth, there may be no apparent fitness costs in some environments.

The interest in quantifying fitness costs is, in large part, due to the influence of fitness costs on the population dynamics of antibiotic-resistant and antibiotic-sensitive bacterial strains [19, 20]. A fitness

¹Department of Biomedical Informatics and Laboratory of Systems Pharmacology, Harvard Medical School, Boston, MA, USA. ²Harvard Data Science Initiative, Harvard University, Boston, MA, USA. ³Present address: Marine and Environmental Sciences, Northeastern University, Boston, MA, USA. ✉email: baym@hms.harvard.edu

Received: 18 May 2021 Revised: 3 March 2022 Accepted: 31 March 2022

Published online: 14 April 2022



cost to antibiotic resistance would slow the spread of resistant strain, as the resistant bacteria would be at a competitive disadvantage [2]. However, it is not straightforward to extrapolate from fitness costs to community composition; several additional dimensions of fitness such as lag time [21], resource

Fig. 1 Conceptual illustration of niche breadth and maximum growth rate as independent dimensions of fitness. Because fitness costs in thermal niche breadth are independent of absolute growth rate, increasing resistance might show a decreased growth rate across all temperatures (cost in maximum growth rate, which occurs at the thermal optimum, T_{opt} ; **A**), a more rapid drop-off in growth rate away from the thermal optimum (cost in thermal niche breadth; **B**), or both a decreased maximum growth rate and a narrower thermal range (cost in both maximum growth rate and niche breadth; **C**).

use efficiency [22], and resource storage [23] also affect competitive outcomes. Thus, while a fitness cost in growth rate represents a deficit in the ability of a strain to quickly reproduce, it is difficult to predict the success of an antibiotic-resistant strain from only these measurements.

In this study, we test the hypothesis that increasing resistance to chloramphenicol carries fitness costs in thermal niche breadth, defined as growth rate across multiple temperatures. We selected chloramphenicol as the focal drug due to its many resistance pathways, which allows us to use genomics to explore the consistency of fitness costs across a variety of genetic mechanisms of resistance [24]. In addition, chloramphenicol resistance spans a large gradient, where evolved MICs (minimum inhibitory concentrations) can be in excess of 100-fold the initial MIC [25]. We evolved resistant bacterial populations by conducting 24 parallel evolution experiments, beginning from a culture of *Escherichia coli* from the Keio collection. We measured the growth rates of these strains at novel temperatures to evaluate how resistance affected thermal tolerance. In addition, we competed strains of varying resistance against one another to investigate how fitness costs of resistance translate to the frequency of genotypes in mixed culture and the competitive success of highly resistant strains. Finally, we sequenced the genomes of isolates from each lineage to understand the genetic basis of resistance and to test whether mutations in specific genes had differential fitness effects in novel temperatures. Together, this study defines thermal niche breadth as a dimension of fitness, quantifies how these fitness costs shape the competitive success of resistant strains, and relates these deficits in novel environments to the genomic basis of resistance.

METHODS

Obtaining resistant strains via experimental evolution

We began with a single liquid culture of the *lacA* knockout (CGSC #11892) from the Keio Collection of single-gene *E. coli* knockouts [26]. We first identified the MIC of this strain ($\sim 3 \mu\text{g}/\text{mL}$) by testing its growth in M9 with varying concentrations of chloramphenicol (Fig. 2). We passaged these cultures at a concentration of $2.5 \mu\text{g}/\text{mL}$ to allow populations to diversify before beginning the selection experiment. We initiated 96 cultures in a 96-well plate, and selected the 24 wells with strongest cell growth to propagate further. Experiments were done using M9 minimal media to preclude biphasic growth arising from multiple potential carbon sources. The cultures were incubated at 37°C with continuous shaking. For each passaging step, the following protocol was used: First, we ensured that all 24 cultures had visible growth. We then passaged one-tenth of the culture to new media containing a chloramphenicol concentration of $\sqrt{2}x$ of the prior concentration. These cultures were allowed to grow for 48 h. If there was not visible growth in all cultures, we passaged the cultures at the same chloramphenicol concentration and allowed cultures to grow for 48 h again.

Cultures were initiated in 96-well plates with $150 \mu\text{l}$ volume, but were moved to 5 mL cultures at timepoint 6, because the small populations were easily extinguished with increasing antibiotic concentrations. As chloramphenicol concentrations became very high ($>50x$ initial MIC), transfers to higher antibiotic concentrations strongly inhibited growth. In the case that there was no visible growth after passaging at the same chloramphenicol concentration, we passaged all cultures in media with no chloramphenicol to restore cell density. Then, we resumed the typical

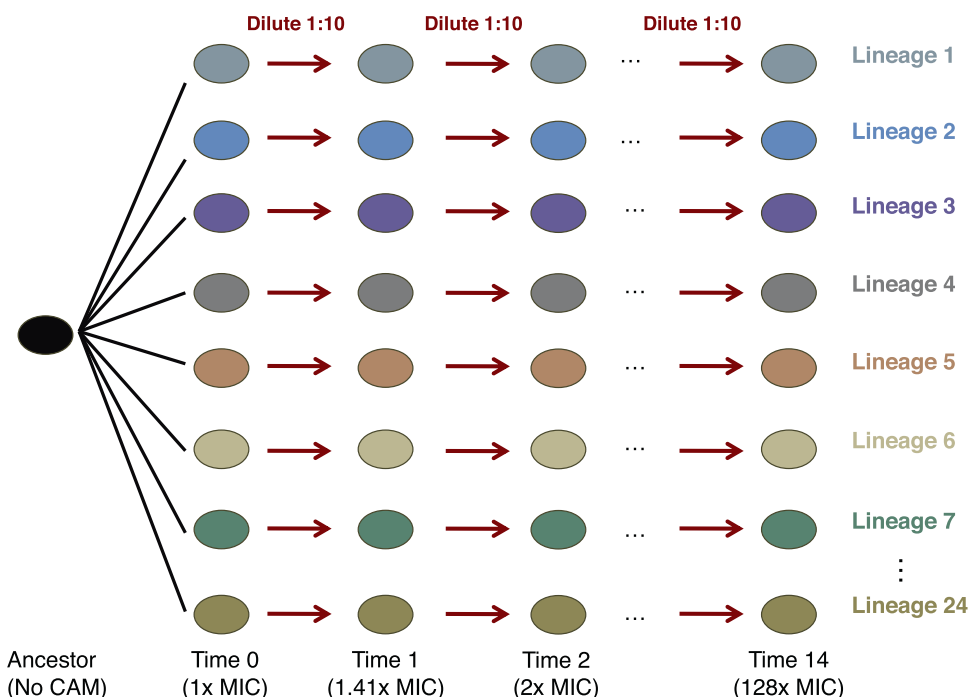


Fig. 2 Schematic of evolution experiment to obtain strains of varying chloramphenicol resistance. Beginning with a common ancestor, grown with no chloramphenicol (CAM), we first passaged cultures at their MIC to create 24 replicate lineages. When transferring cultures to new media, we diluted cultures 1:10 during each passage. The rate of increase in antibiotic was a factor of $\sqrt{2}$ between sequential levels.

protocol steps, beginning at the concentration the cells previously experienced. We terminated the experiment when cultures were no longer able to grow when transferred to a higher chloramphenicol concentration, which occurred after 14 timepoints, representing 128 \times the starting concentration.

Cultures were collected for archival storage immediately before being passaged to media with a greater chloramphenicol concentration. To standardize cell densities for the inoculum, we created saturated cultures by growing 10 μ L of original culture in media with no antibiotic for 48 h, and stored saturated cultures at -80°C in 20% glycerol.

Quantifying fitness: measuring maximal growth rates

We quantified bacterial growth rates by measuring the turbidity of cultures (OD_{600}) using a BioTek Synergy H1 plate reader. We measured 60 cultures per 96-well plate, using only the interior wells of the plate. We used a 96-well pipettor to inoculate 150 μ L of fresh media with 2 μ L of stored culture. Cultures were incubated at a constant temperature for 24 h with continuous shaking, and measurements taken every 5 min. The growth of each culture was measured at three temperatures: their historic temperature of 37°C , and the novel temperatures of 32°C and 42°C . We selected these temperatures by reasoning that the maximum temperature of a mammalian host during fever is $40\text{--}41^\circ\text{C}$, so therefore 42°C would likely induce thermal stress. Then, we selected close 32°C as a symmetric temperature for the lower thermal condition.

The measurement of interest in these experiments was the maximum growth rate achieved by each culture at each of the three temperatures. Some data processing and cleaning was necessary, due to technical variability in the data that arose from two main sources (detailed in Fig. S1). First, there was some spatial variation in initial optical density readings across the 96-well plate, despite using only inner wells. Optical density measurements of blanks were also variable, ranging between 0.09 and 0.11. Second, the small amount of technical noise from the plate reader was disproportionately influential when populations were small, and could artificially inflate calculated growth rates. To address these issues, we first re-centered the optical density data from inoculated wells to have a minimum value of 0.02, indicating a small population at the outset of the measurements. Results of the subsequent analyses were robust to changes in the value selected for the initial optical density (Fig. S2). Then, we used a smoothing function to minimize the effect of discontinuities in optical density measurements, which were generally small but could have disproportionate effects on the data at low optical density values; we

used a local linear model using the surrounding 24 data points to smooth the values. Optical density values were log-transformed before smoothing. Again, results were robust to varying the number of data points included to produce the smoothing (Fig. S2). Finally, to find the maximum growth rate for each sample, we subtracted sequential values after log-transforming and smoothing, and used the maximum difference as the measurement of the maximum growth rate.

We hypothesized that there would be both costs in maximum growth rate and costs in thermal niche breadth as bacteria became more resistant to chloramphenicol. We used a linear regression to evaluate this prediction, where the outcome variables were the growth rates of the cultures (24 lineages \times 14 timepoints \times 3 temperatures = 1008 growth rate measurements) and the predictors were the temperature of measurement (32°C , 37°C , or 42°C), lineage (L1–L24), the timepoint (1 through 14, representing increasing chloramphenicol resistance), and an interaction term between temperature and timepoint. This interaction tests whether the effect of timepoint on growth rate is differentially strong at the three temperatures. In the five instances where there was minimal growth in the cultures (change in $\text{OD}_{600} < 0.05$), we removed the data points from the analysis.

Competing evolved vs. ancestral strains

Next, we wanted to directly evaluate how increasing chloramphenicol resistance influenced competitive ability between ancestral and evolved bacterial strains. This question addresses how the acquisition of antibiotic resistance influences the frequency of the resistant strain in mixed populations. We competed genotypes from the same lineage but different timepoints against each other in the same well of a 96-well plate. The timepoints used for competition experiments were T1, T5, T9, and T13, with all competition experiments done in a pairwise fashion and replicated three times.

We quantified the population sizes of the different strains at the various timepoints via flow cytometry. For each strain used in the competition experiments (24 lineages \times 4 timepoints = 96 strains), we created two transformed strains with either the pCCGi plasmid to express the mCherry protein or the pDiGc plasmid to express the GFP protein. These plasmids confer resistance to ampicillin, and are suited for competition experiments because they are similar plasmids that were constructed by the same research group [27, 28]. We selected one colony from the successful transformations, and created new archived stocks of these strains by growing these strains for 48 h in M9 media containing ampicillin and then storing them at -80°C in 20% glycerol.

For the competition experiments, wells in a 96-well plate were filled with M9 containing ampicillin and were inoculated with 2 μ l of two strains. In each well, there was one strain with the GFP-producing plasmid, and one strain with the mCherry-producing plasmid. Competition experiments were conducted at three temperatures (32 °C, 37 °C, and 42 °C) by incubating the 96-well plate at the given temperature for 24 h with continuous shaking. At 24 h, plates were removed from the incubator, and 6 μ l of each mixed culture was transferred to 200 μ l of water to be read on an LSRII flow cytometer. A minimum of 10,000 cells were counted for each well. The outcome of interest was the population success of the GFP-producing strain; we analyzed the GFP-producing strains, because the population changes were more symmetrically distributed around zero with less skewness. These experiments produced 3456 measurements of population size (4 GFP strains \times 4 mCherry strains \times 3 replicates \times 3 temperatures \times 24 lineages).

Our hypothesis for the competition experiments was that the more resistant strains would fare worse at novel temperatures (32 °C or 42 °C) than in their historical temperature (37 °C). We evaluated this by comparing the fraction of the community comprised of each GFP-transformed strain as a function of the difference in resistance (measured by the difference in the experimental timepoints of the two competing strains). We conducted a linear mixed-effects regression where the outcome variable was the log-ratio of the community comprised by the GFP strain divided by the average fraction of the community comprised by the GFP strain when grown together with the same timepoint with the mCherry plasmid. This standardization accounts for potential differential costs of carrying the GFP vs. mCherry plasmids. A value of 1.4 for the well where lineage 3 T5 containing GFP was competed against lineage 3 T13 mCherry would indicate that the lineage 3 T5 GFP strain comprised 1.4 times the fraction of the community than it did when competed against lineage 3 T5 mCherry strain. The fixed effect variables in the regression included the difference in resistance between strains, temperature, and lineage, with all interaction terms included. The difference in resistance was measured by the difference in the experimental timepoints of the two competing strains. For example, if the GFP-transformed strain were from T5 and the mCherry-transformed strain were from T13, the difference in resistance would be -8 . As such, there are more data points at differences of 4 than 8 or 12, because there are more pairs of strains that are separated by 4 timepoints than are separated by 12 timepoints. A significant interaction between temperature and resistance difference indicates that the effect of resistance on strain growth is different among temperatures. We included a random effect to allow the log-ratio of GFP strains to vary in response to competing against different mCherry strains.

Genomic sequencing to identify genetic basis of resistance

After selecting strains for the competition experiments, we sequenced the GFP-transformed versions of these 96 strains. We followed the protocol set out in [29]; briefly, we extracted genomic DNA using an Invitrogen kit, then carried out tagmentation using the Nextera kit (Illumina). We used Q5 High Fidelity 2 \times Master Mix for the library prep, and cleaned up the libraries with SPRI magnetic beads. We ran the sequencing on a NovaSeq (Illumina) at the Harvard Bauer Core, producing 150 bp paired-end reads. We also sequenced the initial ancestral strain prior to exposure to any antibiotic.

We used the computational pipeline, breseq, to determine mutations arising in each strain [30]. This toolkit was developed for the purpose of analyzing microbial genomes during the course of evolutionary experiments. We used a genome for *E. coli* K-12, substr. MG1655 (#U00096 from Genbank) as the initial reference, which we updated using the data from our sequenced ancestral strain. The output of this pipeline identifies locations of mutations in each genome and specifies the genes in which they occur.

Finally, to examine whether there were differential effects of mutations across the three temperatures, we analyzed whether the location of mutations within each strain could explain the outcome of the competition experiments described above. We used a linear regression where the outcome variable was, again, the log-ratio of the strain in competition divided by the population of the strain when grown against the same timepoint. The predictor variables were the difference between the two strains in the number of mutations in each gene (e.g., L11 T13 has 1 mutation in *marR* and L11 T9 has zero mutations in *marR*, the value for *marR* for L11 T13 is 1). We included interactions between all genes and temperature, in order to test whether estimated effect sizes of mutations differed in the three thermal environments. Also, we included lineage as a predictor variable to account for potential differences in the success of the GFP strains between lineages.

RESULTS

Obtaining bacterial strains with varied resistance levels

We experimentally evolved 24 replicate lineages of *E. coli* to tolerate increasing concentrations of chloramphenicol. By serially passaging bacterial cultures through 14 increasing chloramphenicol levels, we obtained 336 (24 lineages \times 14 concentrations) populations of *E. coli* across a gradient of resistance levels (Fig. 2). The 24 replicate lineages enabled us to study the variability arising from the stochastic nature of mutation acquisition. We refer to these populations as “cultures” rather than “strains” due to the possible coexistence of multiple genotypes.

Resistance incurs costs in both thermal tolerance and maximum growth rate

We measured growth rates of experimentally evolved *E. coli* cultures at three different temperatures: their historic temperature of 37 °C, and the novel temperatures of 32 °C and 42 °C. We hypothesized that growth rate costs of resistance would be larger in the novel temperatures, consistent with reduced thermal niche breadth.

Overall, we found the growth rates decreased strongly with increasing antibiotic resistance (Fig. 3A). We then calculated relative growth rates for each lineage by dividing the growth rate at each timepoint by the growth rate of the culture at timepoint 1 (T1) at the appropriate temperature (e.g., all cultures at 32 °C were standardized by the ancestral growth rate at 32 °C). Analysis of these relative growth rates showed that there was both a fitness cost in maximum growth rate and a fitness cost in thermal niche breadth; the linear model showed a strong negative effect of increasing resistance on growth rate at 37 °C ($F_{1, 974} = 988.2, p < 0.001$), and significant variability in the effect of resistance on growth at the three different temperatures ($F_{1, 974} = 13.8, p < 0.001$).

The negative effect of resistance on growth rate was greater at 32 °C and 42 °C than at 37 °C (Fig. 3B). Thus, there were disproportionate fitness costs in both the novel temperatures. This finding is corroborated by counting the number of evolved (T2 or greater) populations that showed an increased growth rate, when compared with their ancestor (T1); at 37 °C, there were 41 evolved cultures with growth rates greater than that of the ancestor at 37 °C, whereas at 32 °C there were 13 evolved cultures that grew faster than the ancestor at 32 °C, while at 42 °C only two did. Therefore, the presence of fitness costs was more consistent in the novel temperatures.

Strong competitive disadvantage of resistance at increased temperature

Next, we evaluated the effects of increasing chloramphenicol resistance on competitive success, measured by the fraction of the community comprised by a resistant strain when grown in mixed culture with a more sensitive strain. We transformed strains from 96 cultures (timepoints 1, 5, 9, and 13 for each of the 24 lineages) with either GFP or mCherry plasmids and quantified population sizes after competition assays using flow cytometry. We found that resistance level was a strong driver of the composition of mixed cultures in the competition experiments (Fig. 4). For example, at 32 °C and 37 °C, the most sensitive strains (T1) grew to a population 1.3x larger when grown against the most resistant strain (T13), as compared with being grown against the same timepoint (T1). The growth differential was much stronger at 42 °C, where the most sensitive strain (T1) grew to 3x their population size when competed against the most resistant strain (T13).

For each lineage, we evaluated whether the competitive cost of resistance was different at 32 °C or 42 °C when compared with the effect at 37 °C. We found that 12 of the 24 lineages had significantly stronger negative effects of resistance on strain growth at 42 °C, as compared with 37 °C. One lineage (L16) had significantly smaller costs of resistance at 42 °C. There were no lineages where there was a significant difference in the effect of resistance between 37 °C and 32 °C. Full results can be found in

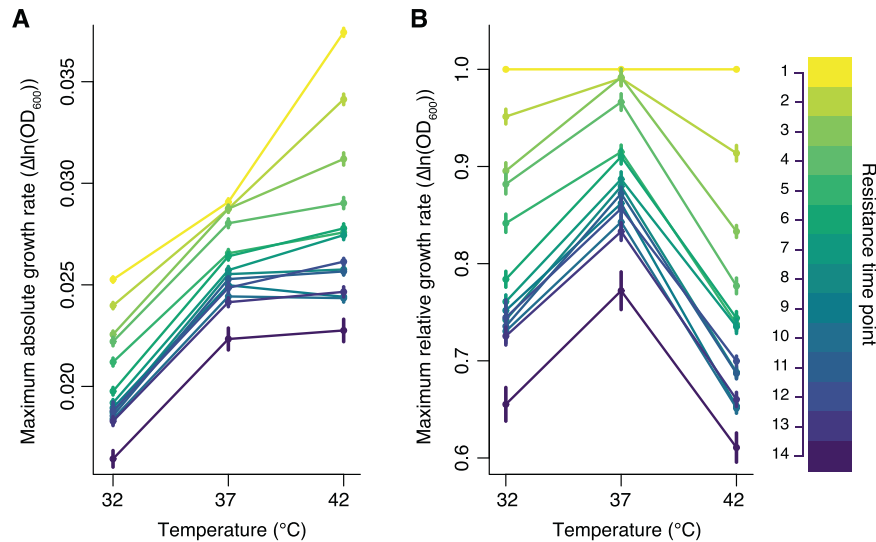


Fig. 3 Strong fitness costs to both thermal niche breadth and maximum growth rate. Absolute growth rates (measured as the maximum difference in sequential log-transformed optical densities) varied across the three temperatures, and were generally highest at 42 °C for a given culture (A). Increasing resistance, as measured by timepoint in the evolution experiment (darker colors indicate higher resistance levels), resulted in reduced maximum growth rates (A). These differences are more apparent when analyzing relative growth rates (i.e. the growth rates divided by the respective ancestral growth at T1 at each respective temperature) (B). As resistance increased, the relative growth rate decreased at 37 °C, but showed even larger declines at the novel temperatures of 32 °C and 42 °C (B). Of the three scenarios depicted in Fig. 1, these findings mirror Fig. 1C, where there are costs to both maximum growth rate and thermal niche breadth. Points show the mean and standard error of growth rates from measurements from each of the 24 lineages.

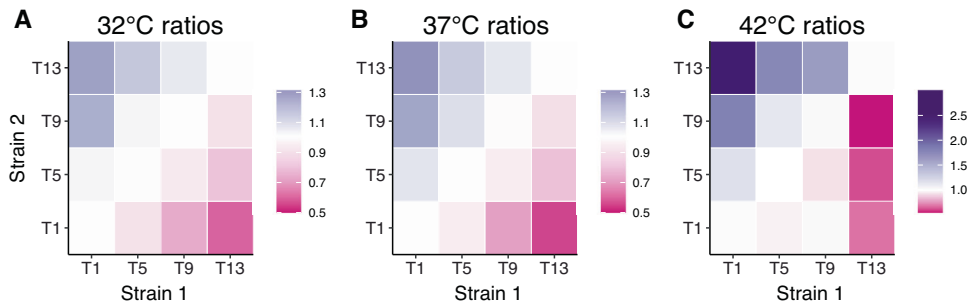


Fig. 4 Resistant strains are outcompeted by their sensitive ancestors in the absence of drug, particularly at the warmer temperature. Heatmaps show the performance of two strains in competition experiments at the 3 temperatures, with cell values giving the mean ratio of a strain's population frequency after competition with another strain vs. competition with itself. The axes are the timepoints from which each strain was sampled. A value of 1 indicates no differential performance. Purple cells (values larger than 1) indicate that Strain 1 out-performed in final community composition, as compared with when that same strain was competed against a strain from the same timepoint, but sampled separately (and labeled with a different fluorophore, mCherry for Strain 2 vs. GFP for Strain 1). In contrast, darker pink cells (values smaller than 1) indicate that the first strain performed worse than in competition with the same timepoint. At 42 °C (C), there was a greater differential in frequencies than at 32 °C or 37 °C (A, B), indicated by the darker colors (note the different scale bars between 42 °C and the other two temperatures).

Table S1. When removing the interaction between temperature and lineage to evaluate the average effect of resistance across all lineages, we found that the effect of resistance differed across temperatures ($F_{2, 3309} = 51.3, p < 0.001$). Specifically, the negative effect was greater at 42 °C than 37 °C (a slope 59% greater at 42 °C), though there was no significant difference between 32 °C and 37 °C (a slope 11% weaker at 32 °C). To visualize these differences in the effect of resistance on strain growth, we show two lineages with contrasting results; lineage 5 had no significant differences in the effect of resistance across temperature, whereas lineage 19 showed a much stronger effect of resistance differences at 42 °C than at the other two temperatures (Fig. 5).

Variability in routes to resistance among lineages

We then sequenced genomes for the 96 strains used in the competition experiments to evaluate how the genetic mechanism

of resistance affected fitness. All samples had coverage of at least 100x, with a minimum number of reads per genome of 2.4 million. Using the genomic data, we identified 220 mutations across these 96 strains; of these mutations, 24 occurred within strains at T1, 44 in strains at T5, 65 in strains at T9, and 87 in strains at T13. We also identified the timepoint at which these mutations were first identified within a lineage. All 24 mutations at T1 were new when comparing against the ancestor, along with 29 mutations present at T5 but not the same lineages at T1, 26 mutations present at T9 but not T5, and 40 mutations present at T13 but not T9. We saw that most mutations fell within genes for known resistance mechanisms, such as efflux pumps, the multiple antibiotic resistance protein (*mar*), or ion channels. We grouped the mutations into 10 categories for further analysis: those associated with the *acr* efflux pump (64 mutations), ATP synthase (42 mutations), the *mar* resistance protein (20 mutations), the *mdfA*

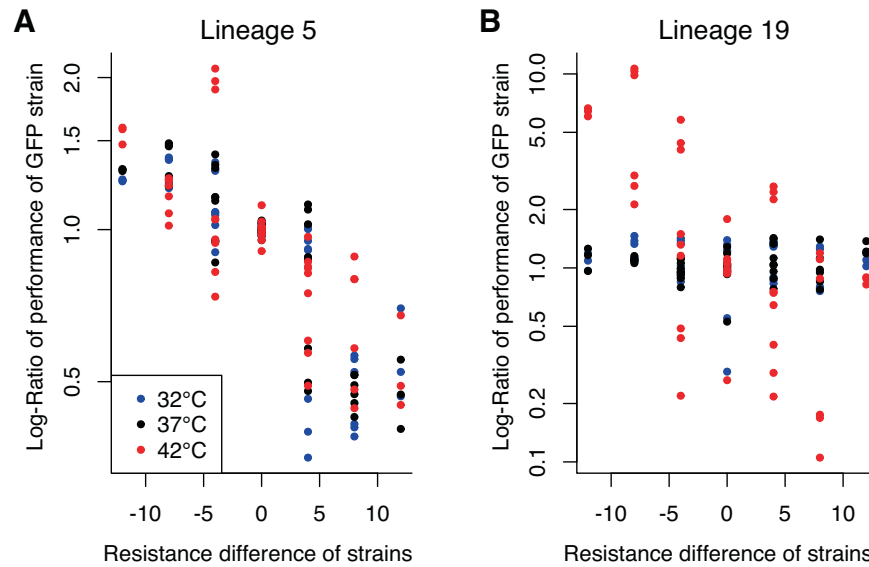


Fig. 5 Lineage-specific fitness costs in thermal tolerance. While many lineages demonstrated a greater cost of resistance at 42 °C than the other two temperatures, some lineages showed no increased effect at the warmer temperature. Lineage 5 (A) is an example of an evolutionary trajectory where fitness costs were not substantially different across temperatures. The x-axis is the difference in experimental timepoints at which strains were collected (a proxy for minimum resistance level). The y-axis gives the change in performance of the GFP strain as compared with competition against the same timepoint. Conversely, lineage 19 (B) shows an example of a strong interactive effect of fitness costs and temperature, where strain performance is more impacted by resistance at 42 °C (red circles) than at the other two temperatures.

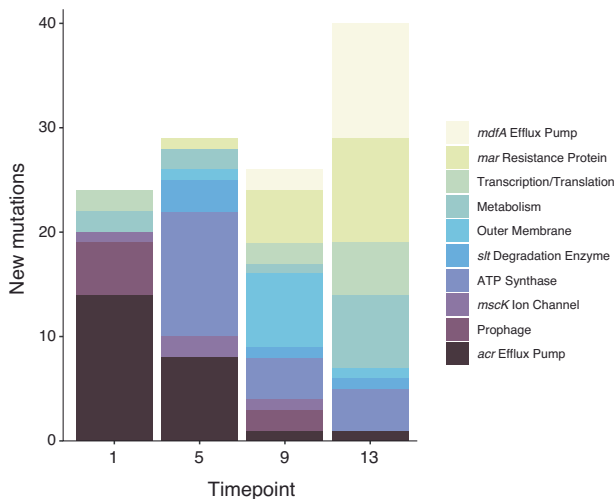


Fig. 6 Transition of resistance strategies across the chloramphenicol gradient. The types of mutations acquired at each timestep changed as antibiotic levels increased. The most common pathways to resistance at the four timepoints were mutations in the *acr* efflux pump (T1), ATP synthase genes (T5), outer-membrane proteins (T9), and the *mdfA* efflux pump (T13).

efflux pump (15 mutations), other metabolism (generally related to carbon usage, 16 mutations), the *mscK* ion channel (12 mutations), outer-membrane-associated proteins (12 mutations), mutations in prophages (15 mutations), *slt* degradation protein (12 mutations), and mutations affecting transcription/translation (12 mutations). We analyzed the dataset containing the first observation of each mutation to assess whether certain mechanisms appeared earlier or later in evolutionary trajectories (Fig. 6). Using chi-squared tests on the number of mutations in each category across the four timepoints, we found that mutations associated with the *acr* efflux pump ($p < 0.001$), ATP synthase ($p = 0.041$), the *mar* resistance protein ($p = 0.022$), outer-membrane proteins ($p = 0.018$), and the *mdfA* efflux pump ($p = 0.013$) were nonrandomly

distributed across evolutionary time. Specifically, early mutations at T1 were disproportionately located within the *acr* efflux pump, while mutations at T5 were often within the *acr* efflux pump and associated with ATP synthase. At T9, mutations within the outer-membrane proteins became more common. Finally, the most resistant strains frequently had mutations in the *mar* resistance protein and the *mdfA* efflux pump. Although conducting 10 chi-squared tests for the 10 categories allows the possibility of finding spurious positive results, the probability of spuriously identifying five categories at a threshold of $p < 0.05$ is < 1 in 16,000.

Fitness effects of resistance mutations are more extreme at higher temperature

We calculated the estimated effect of mutations in 37 genes on the outcomes of the pairwise competition experiments, as to compare the distribution of mutational fitness effects across the three temperatures. Many of these genes were part of the same cassettes (e.g., *acrA*, *acrB*, and *acrR*). Initially, we identified mutations in 43 genes, though the distribution of mutations in 6 of these genes (*yejA*, *yfaQ*, *xdhB*, *rplD*, *rpoC*, and *uvrA*) were equivalent to the mutation occurrence of other genes, and thus could not be included in the analyses due to the fact that the predictor variables were identical. Of these remaining 37 genes, we saw significant differences in the estimated effects of mutations in 24 genes between 37 °C and 42 °C. Conversely, there were zero significant differences in effect size between the temperatures of 32 °C and 37 °C. Effect sizes in this analysis signify the difference in the success of a strain as a result of carrying one extra mutation in the indicated gene. Then, we evaluated whether the range of gene effects was larger at 42 °C or 32 °C, as compared with the range of gene effects at 37 °C (Fig. 7). We conducted F-tests on the distribution of gene effect sizes at 37 °C vs. 42 °C and at 37 °C vs. 32 °C to find whether the variances of these distributions were unequal. We found that the range of gene effects was greater at 42 °C than 37 °C ($F_{36, 36} = 5.68$, $p < 0.001$) but that the range of gene effects was not different between 32 °C and 37 °C ($F_{36, 36} = 0.91$, $p = 0.79$).

The genes with the most significant additional fitness cost at 42 °C were: *mscK*, *opgH*, *dgcF*, *atpD*, *uvrA/ssb*, and *ssb*. Of these,

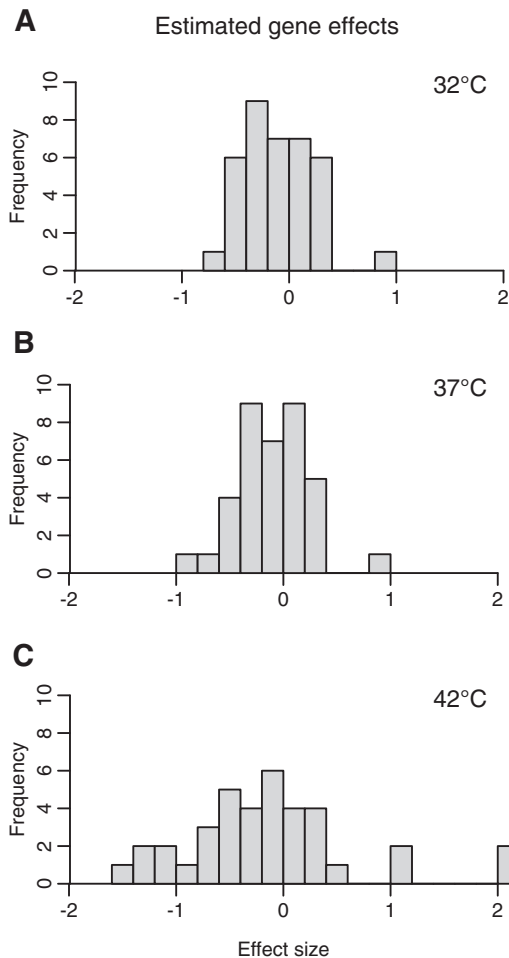


Fig. 7 Effects of mutations are more extreme at a warmer temperature. Results of the linear regression quantifying the effects of mutations within 37 genes show that the estimated impact of mutations is greatest at 42 °C, as compared with 32 °C or 37 °C. Values in histograms are the coefficients from the linear model, where each coefficient is the estimated effect of a gene-specific mutation on the ratio of that strain in competition. Effect sizes near zero indicate no effect, whereas an effect size of 1 indicates a one-log-fold increase in the competitive success of a strain that has acquired a mutation in the given gene. The variance of effect sizes at 42 °C is significantly greater than at the other two temperatures.

only mutations in *atpD* and *mscK* were common, appearing in more than 1 lineage. These genes are involved in ATP synthesis and in ion transport via the mechanosensitive channel MscK, respectively.

Finally, we combined the competition data with the genomic data to examine whether specific categories of mutations were more likely to result in decreased thermal tolerance. For this analysis, we used Fisher's Exact Tests to determine whether lineages with a greater cost of resistance at 42 °C (12 lineages) were more likely to have any specific type of mutation (using the 10 mutation categories shown in Fig. 5). Surprisingly, of these 10 tests, we found no significant ($p < 0.05$) associations between mutation type and the presence of fitness costs to thermal niche breadth, suggesting that the tradeoff is not tied to a specific mechanism of resistance.

DISCUSSION

The results of our experiments show strong evidence for a narrowing of thermal tolerance as a trade-off of antibiotic resistance. Specifically, fitness costs in growth rate were greater

in novel temperatures (32 °C and 42 °C) than at the historic temperature of 37 °C, indicating that resistant bacteria are less competitively fit in these new environments (Figs. 3 and 4). When considering measurements across all three temperatures, fitness costs were detected in every strain with an MIC at least twice that of the ancestor. Trade-offs to antibiotic resistance are particularly strong at 42 °C, where population dynamics appear qualitatively different than 37 °C and 32 °C. At 42 °C, costs in growth rate were nearly ubiquitous among lineages, and resistant strains composed a much smaller fraction of community composition in the competition experiments. Interestingly, no single genetic strategy of resistance seemed more likely to cause this decreased thermal tolerance, suggesting that this fitness cost might be generalizable to other antibiotics with different resistance mechanisms. Although the growth rate and competition experiments were largely concordant, there were minor differences in the effects of lower temperature on apparent fitness costs, which may be explained by several factors. First, there are possibly multiple coexisting strains in growth rate cultures, but only one genotype was selected for the competition experiments. Noting the large spread in the effect of resistance mutations on fitness (Fig. 7), the outcome of competition experiments depends on the specific genotypes, in addition to the resistance level. Second, as noted previously, additional factors such as resource use efficiency and resource uptake rates also affect eventual population size. Furthermore, we found it notable that the thermal optimum of the ancestor was closest to 42 °C than it was to the historic temperature of 37 °C. While we lack an explanation for the mismatch in thermal optimum and historic growth conditions, the results demonstrate empirically the independence of the maximum growth rate and niche breadth; although the thermal optimum was nearer to 42 °C than 37 °C, there was a greater cost in relative fitness at 42 °C than 37 °C. Overall, our experiments demonstrate that chloramphenicol resistance reduces the ability of evolved cells to grow in novel thermal environments, and that these trade-offs put resistant strains at a strong competitive disadvantage at warmer temperatures.

Despite the strong overall pattern that resistant strains fared poorly at higher temperatures relative to their ancestor, there was substantial variation between lineages in this effect. There are many variables that could mediate the fitness costs across lineages, though the most obvious is that the stochastic accumulation of mutations leads to varied genetic bases of resistance with varied costs in new environments [31]. Thus, future experiments studying the trade-offs in novel environments should include a high degree of replication in order to determine the probability of such costs existing in a single lineage. There are additional experimental factors that could interact with this stochasticity of evolutionary trajectories, including population size and the strength of the selection gradient. At very large population sizes, convergence of evolutionary trajectories becomes more likely due to mutation saturation within populations [32]; in this case, the most strongly beneficial mutations arise in each population, and will persist. We can be sure that these experiments did not approach mutation saturation because only one lineage evolved the strongly beneficial media adaptation in *araD*. This mutation can be clearly seen as a positive outlier in the estimated gene effect sizes at 37 °C, yet it only appeared once (Fig. 7). Similarly, the strength of the selection gradient determines the fraction of the population that can survive passaging to a higher antibiotic concentration. At stronger selection gradients, fewer genotypes would survive the incremental increase in antibiotic, leading to a smaller number of genetic routes to resistance [33]. Thus, the initial population heterogeneity, as well as the subsequent bottleneck size, may influence the presence and variation in evolutionary trade-offs. Furthermore, the particular media and antibiotic used also influence the distribution of fitness costs, as the variety of carbon sources and the specific

antibiotic targets also determine the number and type of mutations conferring fitness advantages. In these specific experiments, observed trade-offs may also be confounded by adaptation to the minimal media over the course of the evolution experiment, in addition to the adaptations to increasing antibiotic resistance. However, the small number of mutations in metabolic pathways makes us confident that this is a strong factor in our results. Finally, it would also be interesting to evaluate whether structural variation in genomes (such as duplications or inversions) or changes to transcriptional regulation correspond to the observed fitness costs, as our present sequencing methodologies cannot address these possibilities.

Two components of our analyses suggest potential mechanisms leading to decreased thermal niche breadth: the mutations involved in the genetic basis of resistance, and the result that warmer temperatures are more detrimental to resistant bacteria relative to sensitive. Increased temperatures have a multitude of effects on bacterial physiology, including increased membrane fluidity [34], altered protein folding [35], reduced generation time [36], and increased speed of chemical reactions [37]. These effects of temperature might interact with specific mechanisms of resistance to yield the disproportionate fitness costs. For example, many proteins involved in resistance are embedded within the outer membrane, such as efflux pumps and outer-membrane porins. The efficacy of these resistance mechanisms, or the energy needed for these complexes to function, might change as a function of membrane fluidity. A higher temperature could also increase cell susceptibility to antibiotics, as altered protein folding at this temperature might expose additional chloramphenicol targets within ribosomes. In this case, cells might need to upregulate activity of resistance mechanisms to produce the same level of resistance. Alternatively, the location of mutations within proteins might be more detrimental at 42 °C due to altered protein structure. Furthermore, the ATP synthase mutations that were observed may confer resistance by slowing cellular metabolism sufficiently that chloramphenicol targets are no longer active; this is frequently seen in persister cells [38], and persister mutations are common in early stages of resistance evolution [39]. It is possible that there is a greater cost of these ATP synthase mutations at 42 °C, as higher temperatures often require increased cellular metabolism and respiration. Finally, the rapid drop-off in activity of many enzymes above their thermal optimum [40] means that cells may be particularly sensitive to perturbations near the upper bound of their thermal range (e.g., Fig. 1). Thus, a resistance mutation that changes the enzyme kinetics by a small amount would have the greatest effect near this upper thermal limit.

When determining how to place a quantitative measurement on the conceptual notion of niche breadth, there are multiple possible metrics that could be used [41]. Here, we chose to measure niche breadth as the relative growth rate of evolved strains against their ancestors, because it reflects the importance of strain competition in antibiotic resistance evolution. Indexing the growth rate against that of its ancestral strain is a strong predictor of the ability of the mutants to increase in abundance by outcompeting the ancestral strains [8, 42]. As such, using the relative growth rate as a measurement of niche breadth implicitly indicates that interactions with other cells are important in shaping niche breadth. Thus, our measurements of niche breadth correspond more closely to quantifying the “realized niche,” which includes the effect of biotic interactions on population persistence, as compared with the “fundamental niche” of abiotic conditions the organism can tolerate [43]. Conversely, the fundamental niche may be of greater interest in contexts where community composition is variable, or where range boundaries are driven by upper or lower temperature limits. In this context, a more appropriate measurement of niche breadth might be obtained by calculating the width or area of the thermal performance curve [44, 45]. Thus, it is unlikely that any single quantitative metric of niche breadth would be appropriate for every population of interest.

Deciding upon the definition of niche breadth for an experimental system requires understanding the relative importance of biotic interactions, abiotic conditions, and the components of fitness that contribute to maintaining a viable population.

In addition to thermal tolerance, there are many other dimensions of niche breadth where fitness costs could manifest. Further exploration of environmental tolerance might include the ability to withstand desiccation or changes in pH. Another aspect of decreased niche breadth could be the ability to survive biotic interactions, such as the ability to evade a wide variety of immune system responses or to avoid infections by bacteriophages. Of particular importance are trade-offs that would manifest in reduced virulence. This category of fitness costs to niche breadth might include reduced host range or decreased survival outside the human body. These two dimensions of fitness would slow the spread of person-to-person infection by either decreasing the number of susceptible hosts or decreasing the transmission rate of an infected individual. Thus, further studies of evolutionary fitness costs might explicitly incorporate multiple stages of a pathogen’s life cycle. More broadly, the need to simultaneously maintain adaptations under antibiotic pressure reflects the pressures of a generalist vs. specialist strategy. Theory indicates that it might be difficult to evolve strong specialization (e.g., antibiotic resistance) without losing other functionality due to pleiotropic effects [46]. Because the long-term survival of resistant populations is the multiplicative effect of survival across different life stages, modest trade-offs in niche breadth could strongly impact the population dynamics of resistant bacteria.

Given the impact of costs to niche breadth on the frequency of resistant bacteria, these trade-offs likely have consequences for the long-term evolution of antibiotic resistance. For example, if narrower niche breadth means that resistance can change from beneficial to detrimental over short time spans (as is the case when changing environments), this rapid reversal in fitness could select for easy gain and loss of resistance. Indeed, this is seen frequently in bacteria, when resistance in nature can be nearly instantaneously acquired by horizontal gene transfer or transposable elements [47]. In addition, these experiments suggest that there are further dimensions of bacterial fitness that have not been tested by laboratory experiments, due to the homogenous environments used for cell culturing. Testing for fitness costs in novel environments could shed light on the temporal or spatial distribution of resistance evolution. For example, the finding that resistance decreases thermal niche breadth might contribute to the observation that resistance increases with ambient temperature [48]. Similarly, because some mechanisms of antibiotic resistance overlap with physiological temperature shock responses [49], the distribution of antibiotic-resistant bacteria may shift as climate change intensifies [50]. Consequently, these experiments raise the question of how adaptation for resistance interacts with adaptation to other specific stressors, and whether fitness effects across different environments are correlated (e.g., [51]). For example, it would be both clinically and theoretically valuable to know whether antibiotic resistance is lost more readily when cells are subjected to novel selective pressures. More broadly, integrating niche breadth into the framework of fitness costs has the potential to resolve seeming contradictions in resistance evolution; costs in niche breadth allow for the possibility that any resistance mutation has trade-offs, but the costs may not be apparent in a constant environment.

REFERENCES

1. Chatterjee A, Modarai M, Naylor NR, Boyd SE, Atun R, Barlow J, et al. Quantifying drivers of antibiotic resistance in humans: a systematic review. *Lancet Infect Dis.* 2018;18:e368–e378.
2. Andersson DI, Hughes D. Antibiotic resistance and its cost: is it possible to reverse resistance? *Nat Rev Microbiol.* 2010;8:260–71.

3. Law R. Optimal life histories under age-specific predation. *Am Nat.* 1979;114:399–417.
4. Luciani F, Sisson SA, Jiang H, Francis AR, Tanaka MM. The epidemiological fitness cost of drug resistance in *Mycobacterium tuberculosis*. *Proc Natl Acad Sci USA.* 2009;106:14711–5.
5. El Meouche I, Dunlop MJ. Heterogeneity in efflux pump expression predisposes antibiotic-resistant cells to mutation. *Science.* 2018;362:686–90.
6. Wood KB, Cluzel P. Trade-offs between drug toxicity and benefit in the multi-antibiotic resistance system underlie optimal growth of *E. coli*. *BMC Syst Biol.* 2012;6:1–1.
7. Durão P, Balbontin R, Gordo I. Evolutionary mechanisms shaping the maintenance of antibiotic resistance. *Trends Microbiol.* 2018;26:677–91.
8. Melnyk AH, Wong A, Kassen R. The fitness costs of antibiotic resistance mutations. *Evol Appl.* 2015;8:273–83.
9. Gagneux S, Long CD, Small PM, Van T, Schoolnik GK, Bohannan BJM. The competitive cost of antibiotic resistance in *Mycobacterium tuberculosis*. *Science.* 2006;312:1944–6.
10. Lin W, Zeng J, Wan K, Lv L, Guo L, Li X, et al. Reduction of the fitness cost of antibiotic resistance caused by chromosomal mutations under poor nutrient conditions. *Environ Int.* 2018;120:63–71.
11. Sander P, Springer B, Prammananant T, Sturfels A, Kappler M, Pletschette M, et al. Fitness cost of chromosomal drug resistance-conferring mutations. *Antimicrob Agents Chemother.* 2002;46:1204–11.
12. Olivares J, Álvarez-Ortega C, Martínez JL. Metabolic compensation of fitness costs associated with overexpression of the multidrug efflux pump MexEF-OprN in *Pseudomonas aeruginosa*. *Antimicrob Agents Chemother.* 2014;58:3904–13.
13. Fang FC, Frawley ER, Tapscott T, Vázquez-Torres A. Discrimination and integration of stress signals by pathogenic bacteria. *Cell Host Microbe.* 2016;20:144–53.
14. Runkel S, Wells HC, Rowley G. Living with stress: a lesson from the enteric pathogen *Salmonella enterica*. *Adv Appl Microbiol.* 2013;83:87–144.
15. Hasday JD, Fairchild KD, Shanholtz C. The role of fever in the infected host. *Microbes Infect.* 2000;2:1891–904.
16. Berger CN, Sodha SV, Shaw RK, Griffin PM, Pink D, Hand P, et al. Fresh fruit and vegetables as vehicles for the transmission of human pathogens. *Environ Microbiol.* 2010;12:2385–97.
17. Mondal S, Pathak BK, Ray S, Barat C. Impact of P-Site tRNA and antibiotics on ribosome mediated protein folding: studies using the *Escherichia coli* ribosome. *PLoS One.* 2014;9:e101293.
18. Wilson DN. Ribosome-targeting antibiotics and mechanisms of bacterial resistance. *Nat Rev Microbiol.* 2014;12:35–48.
19. Levin BR, Lipsitch M, Perrot V, Schrag S, Antia R, Simonsen L, et al. The population genetics of antibiotic resistance. *Clin Infect Dis.* 1997;24:59–16.
20. Mortimer TD, Pathela P, Crawley A, Rakeman JL, Lin Y, Harris SR, et al. The distribution and spread of susceptible and resistant *Neisseria gonorrhoeae* across demographic groups in a major metropolitan center. *Clin Infect Dis.* 2021;73:e3146–e3155.
21. Adkar BV, Manhart M, Bhattacharyya S, Tian J, Musharbash M, Shakhnovich EI. Optimization of lag phase shapes the evolution of a bacterial enzyme. *Nat Ecol Evol.* 2017;1:149.
22. Hodapp D, Hillebrand H, Striebel M. “Unifying” the concept of resource use efficiency in ecology. *Front Ecol Evol.* 2019;6.
23. de Mazancourt C, Schwartz MW. Starve a competitor: evolution of luxury consumption as a competitive strategy. *Theor Ecol.* 2012;5:37–49.
24. Crofts TS, Sontha P, King AO, Wang B, Biddy BA, Zanolli N, et al. Discovery and characterization of a nitroreductase capable of conferring bacterial resistance to chloramphenicol. *Cell Chem Biol.* 2019;26:559–570. e6
25. Toprak E, Veres A, Michel J-B, Chait R, Hartl DL, Kishony R. Evolutionary paths to antibiotic resistance under dynamically sustained drug selection. *Nat Genet.* 2012;44:101–5.
26. Baba T, Ara T, Hasegawa M, Takai Y, Okumura Y, Baba M, et al. Construction of *Escherichia coli* K-12 in-frame, single-gene knockout mutants: the Keio collection. *Mol Syst Biol.* 2006;2:2006.0008.
27. Figueira R, Watson KG, Holden DW, Helaine S. Identification of salmonella pathogenicity island-2 type III secretion system effectors involved in intramacrophage replication of *S. enterica* serovar typhimurium: implications for rational vaccine design. *MBio.* 2013;4:e00065.
28. Helaine S, Thompson JA, Watson KG, Liu M, Boyle C, Holden DW. Dynamics of intracellular bacterial replication at the single cell level. *Proc Natl Acad Sci USA.* 2010;107:3746–51.
29. Baym M, Kryazhinskiy S, Lieberman TD, Chung H, Desai MM, Kishony R. Inexpensive multiplexed library preparation for megabase-sized genomes. *PLoS One.* 2015;10:e0128036.
30. Deatherage DE, Barrick JE. Identification of mutations in laboratory-evolved microbes from next-generation sequencing data using breseq. *Methods Mol Biol.* 2014;1151:165–88.
31. Kassen R, Bataillon T. Distribution of fitness effects among beneficial mutations before selection in experimental populations of bacteria. *Nat Genet.* 2006;38:484–8.
32. Szendro IG, Franke J, de Visser JAGM, Krug J. Predictability of evolution depends nonmonotonically on population size. *Proc Natl Acad Sci USA.* 2013;110:571–6.
33. Wistrand-Yuen E, Knopp M, Hjort K, Koskiniemi S, Berg OG, Andersson DI. Evolution of high-level resistance during low-level antibiotic exposure. *Nat Commun.* 2018;9:1–12.
34. de Mendoza D, Cronan JE Jr. Thermal regulation of membrane lipid fluidity in bacteria. *Trends Biochem Sci.* 1983;8:49–52.
35. Chowdhury S, Maris C, Allain FH-T, Narberhaus F. Molecular basis for temperature sensing by an RNA thermometer. *EMBO J.* 2006;25:2487–97.
36. Ratkowsky DA, Olley J, McMeekin TA, Ball A. Relationship between temperature and growth rate of bacterial cultures. *J Bacteriol.* 1982;149:1–5.
37. Ratkowsky DA, Olley J, Ross T. Unifying temperature effects on the growth rate of bacteria and the stability of globular proteins. *J Theor Biol.* 2005;233:351–62.
38. Lewis K. Persister cells and the riddle of biofilm survival. *Biochem (Mosc).* 2005;70:267–74.
39. Windels EM, Michiels JE, Fauvert M, Wenseleers T, Van den Bergh B, Michiels J. Bacterial persistence promotes the evolution of antibiotic resistance by increasing survival and mutation rates. *ISME J.* 2019;13:1239–51.
40. Elias M, Wieczorek G, Rosenne S, Tawfik DS. The universality of enzymatic rate-temperature dependency. *Trends Biochem Sci.* 2014;39:1–7.
41. Gvozdik L. Just what is the thermal niche? *Oikos.* 2018;127:1701–10.
42. Gullberg E, Cao S, Berg OG, Illbäck C, Sandegren L, Hughes D, et al. Selection of resistant bacteria at very low antibiotic concentrations. *PLoS Pathog.* 2011;7:e1002158.
43. Hutchinson GE. Concluding remarks. *Cold Spring Harbor Symp.* 1957, pp. 415–427.
44. Huey RB, Stevenson RD. Integrating thermal physiology and ecology of ectotherms: A discussion of approaches. *Am Zool.* 1979;19:357–66.
45. Comeault AA, Wang J, Tittes S, Isbell K, Ingleby S, Hurlbert AH, et al. Genetic diversity and thermal performance in invasive and native populations of African fig flies. *Mol Biol Evol.* 2020;37:1893–906.
46. Bono LM, Draghi JA, Turner PE. Evolvability costs of niche expansion. *Trends Genet.* 2020;36:14–23.
47. Partridge SR, Kwong SM, Firth N, Jensen SO. Mobile genetic elements associated with antimicrobial resistance. *Clin Microbiol Rev.* 2018;31:e00088–17.
48. MacFadden DR, McGough SF, Fisman D, Santillana M, Brownstein JS. Antibiotic resistance increases with local temperature. *Nat Clim Chang.* 2018;8:510–4.
49. Cruz-Loya M, Kang TM, Lozano NA, Watanabe R, Tekin E, Damoiseaux R, et al. Stressor interaction networks suggest antibiotic resistance co-opted from stress responses to temperature. *ISME J.* 2019;13:12–23.
50. Rodríguez-Verdugo A, Lozano-Huntelman N, Cruz-Loya M, Savage V, Yeh P. Compounding effects of climate warming and antibiotic resistance. *iScience.* 2020;23:101024.
51. Kinsler G, Geiler-Samerotte K, Petrov DA. Fitness variation across subtle environmental perturbations reveals local modularity and global pleiotropy of adaptation. *Elife.* 2020;9:e61271.

ACKNOWLEDGEMENTS

We thank Anurag Limdi, Eleanor Rand, and Karel Brinda for their constructive comments. Flow cytometry analyses were conducted at the Harvard Medical School Systems Biology FACS facility. This work was supported by the NIH NIGMS award R35GM133700, the David and Lucile Packard Foundation, the Pew Charitable Trusts, and the Alfred P. Sloan Foundation. C.H. was partially supported by the Harvard Data Science Initiative.

AUTHOR CONTRIBUTIONS

C.H. and M.B. designed the project, analyzed and interpreted the data, and wrote the manuscript. C.H. performed the experiments.

COMPETING INTERESTS

The authors declare no competing interests.

ADDITIONAL INFORMATION

Supplementary information The online version contains supplementary material available at <https://doi.org/10.1038/s41396-022-01235-6>.

Correspondence and requests for materials should be addressed to Michael Baym.

Reprints and permission information is available at <http://www.nature.com/reprints>

Publisher's note Springer Nature remains neutral with regard to jurisdictional claims in published maps and institutional affiliations.



Open Access This article is licensed under a Creative Commons Attribution 4.0 International License, which permits use, sharing, adaptation, distribution and reproduction in any medium or format, as long as you give appropriate credit to the original author(s) and the source, provide a link to the Creative Commons license, and indicate if changes were made. The images or other third party material in this article are included in the article's Creative Commons license, unless indicated otherwise in a credit line to the material. If material is not included in the article's Creative Commons license and your intended use is not permitted by statutory regulation or exceeds the permitted use, you will need to obtain permission directly from the copyright holder. To view a copy of this license, visit <http://creativecommons.org/licenses/by/4.0/>.

© The Author(s) 2022